

Laboratory of Physical Chemistry, Eindhoven University of Technology,
P.O. Box 513, 5600 MB Eindhoven, The Netherlands.

Abstract

It is shown that the phenomenon of decarburisation in the CVD of TiC on steel or cemented carbide can be profitably described using diffusion paths on the ternary phase diagram cross sections. Various stages of TiC_{1-x} growth are related to different textures in the coating.

TiC_{1-x} compositions can be determined very precisely by electron probe microanalysis, after special adaptation of the correction program for light element work.

In CVD layers of TiC_{1-x} and in equilibrated diffusion couples containing TiC_{1-x} there is a preferential composition containing 47 respectively 45 at.% carbon. As shown by various analytical techniques this composition is the most stable one, and the one containing a minimum of lattice defects.

Introduction

In 1982 we started a research program with the aim of studying the kinetics of TiC_{1-x} formation on steel and on cemented carbide substrates by CVD (using $TiCl_4/CH_4/H_2$), in relation to the diffusion processes involved in TiC_{1-x} growth (at a temperature of 1273K). First results on CVD experiments were reported in 1983, mainly considering kinetical issues: it was shown that diffusion of carbon atoms in the TiC coating is rate-limiting for CVD experimental conditions without carbon source in the gas phase (1). In a following publication (2), the role of carbon diffusion in the formation of titanium carbide was more elaborately investigated.

In this paper we wish to give an overview of more recent results with emphasis on composition-bonding-diffusion relationships in TiC_{1-x} .

All data referring to preparation procedures and experimental conditions have been described earlier (1,2).

Phase diagram sections and diffusion paths

In our investigations we started with substrates containing no more than two elements, viz. $Fe_{100-y}C_y$ and $Co_{100-y}C_y$. This simplifying approach has the advantage that, after deposition of the TiC_{1-x} layer, a ternary system has been developed, so that use can be made of the appropriate ternary phase diagram sections (in situations assuming thermodynamical equilibrium). At this moment we are extending our research efforts from the ternary systems Fe-Ti-C and Co-Ti-C to the quaternary systems Fe-Cr-Ti-C and Co-W-Ti-C, linking up with the CVD practice of coating steels or cobalt-based cemented carbide substrates with TiC_{1-x} .

The determination of phase relations and the resulting phase diagram cross sections in the systems Fe-Ti-C and Co-Ti-C at 1273K have been published elsewhere (3,4). To study diffusional interactions between phases in ternary systems so-called diffusion paths can be plotted on isothermal cross sections. A diffusion path represents the average concentration profile (as, in our case, determined by electron probe microanalysis) of the various elements in the diffusion zone, and gives information concerning the phenomenology (i.e. morphology and composition) of diffusion layers in solid-state reactions. Diffusion paths do not, however, give direct information of kinetic nature. For the construction of diffusion

paths we followed the general rules proposed by Kirkaldy and Brown (5) and conventionalized by Clark (6).

To construct diffusion paths solid-state diffusion couples have been used as model experiments for CVD-treated samples. Their excellent suitability for simulation purposes has already been demonstrated (4). In this paper we will only present diffusion paths for the Fe-Ti-C system; for similar results on Co-Ti-C we refer to (3). In figs. 1 and 2 observed diffusion paths for diffusion couples of the type $\text{Ti-Fe}_{100-y}\text{C}_y$ are shown. Note, that only in case the iron contains more than 6.5 at.% carbon, a closed TiC_{1-x} layer is formed. When less carbon atoms are present, Fe-Ti intermediate phases are observed, which can contain TiC precipitates; this is shown by the diffusion path in fig. 1.

The diffusion process involved in TiC_{1-x} formation, namely decarburisation of the $\text{Fe}_{100-y}\text{C}_y$ material, is illustrated in fig. 3. The diffusion path in fig. 3 for the case $y > 6.5$ at.% actually is a normal composition profile, determined by measuring concentrations in the one-phase $\text{Fe}_{100-y}\text{C}_y$ material. In case of a two-phase material, however, a profile based on point measurements by EPMA (which, for this case, has already been published earlier (2)) only gives information on the composition in both phases, but not on the number of precipitates as a function of distance. This number decreases strongly in the direction of the TiC_{1-x} reaction layer (fig. 3), showing the decarburisation of the $\text{Fe}_{100-y}\text{C}_y$ starting material. So composition profiles in multiphase materials obtained by point measurements do not reveal information on diffusion phenomena such as decarburisation. For that purpose the use of composition profiles, which are averaged over the observed phases, is indispensable. A diffusion path is then obtained (per definition) by plotting the average composition profile on a phase diagram cross section, omitting the kinetic information.

Conclusion: the various aspects of decarburisation can be profitably studied in a synthesis of diffusion path and composition profile determinations.

TiC_{1-x} growth kinetics in CVD experiments in relation to texture

In chemical vapour deposited TiC_{1-x} almost invariably some sort of preferred growth direction (texture) is being observed. The occurrence of preferred orientation of diffusion-grown crystallites has drawn little attention so far, although important information concerning e.g. different growth mechanisms, (re)crystallization processes or stress-development in coatings can be induced from texture studies (7,8). Furthermore, the occurrence of a preferent growth direction can cause anisotropies in the chemical, physical and mechanical properties of a material (9).

X-ray diffraction was used to identify planes of preferred orientation in the TiC_{1-x} surface layers. To that purpose we combined results by a texture goniometer (Siemens), which plotted pole figures (10), and by a cylindrical camera (Elliot Ltd.) (11).

Observed textures were different for TiC_{1-x} coated $\text{Fe}_{100-y}\text{C}_y$ substrates using a deposition prcess with or without carbon source (CH_4) in the gas phase. If the gas phase contained no carbon source a (110) fibre texture was found, whereas in the case of CH_4 present a (110) fibre texture together with another texture component was found. Because of the relatively weak texture strength it was not easy to discriminate between the possible directions for that second component, (321), (210) and (211), but eventually, on the basis of many pole figures, we may conclude that (321) texture is most probable. As to the relation found between texture sharpness and substrate carbon content we must refer to a previous publication (1). The iron-carbon substrates used in this investigation were texture-

less.

To see whether the (321) plane of preferred orientation was present in the entire coating, TiC_{1-x} grown with CH_4 in the gas phase was slowly grinded off using diamond grinding wheels. The observed X-ray diffraction pattern after each grinding stage is shown in fig. 4. After removal of half of the layer thickness the second texture component has completely disappeared. Only the (110) preferent orientation is remaining, and also a (100) direction has shown up, which is probably a stress-induced texture, generated by the grinding procedure.

From these observations and from the fact that TiC_{1-x} grown without carbon in the gas phase is only showing a (110) texture, it may be supposed that the (321) component is related to a growth process involving carbon from the gas phase, whereas the (110) plane is a texture related to carbon diffusion from the substrate. This supposition is in accordance with the observation cited by Bunshah (12), that the presence of a (reactive) gas in deposition technologies tends to shift the preferred orientation of the coating to higher index planes.

The composition of TiC_{1-x} grown by CVD and by diffusion couple techniques

Many physical properties of TiC_{1-x} , e.g. the hardness, are directly related to the composition of the material. An optimalization procedure of TiC_{1-x} properties by changing CVD process conditions could be performed on the basis of TiC_{1-x} composition determinations. We are now able to measure TiC_{1-x} compositions very accurately in (carefully polished) cross sections of coatings by electron probe microanalysis (EPMA), thanks to a correction program which was specially adapted for ligh element determinations and the specific problems connected with that (13,14). In CVD coatings of TiC_{1-x} another special problem had to be solved, which was caused by the presence of Fe and Cr containing impurities, probably $(Fe,Cr)_3C$ precipitates in the TiC_{1-x} layer. These impurities influence the carbon measurement by EPMA in two different ways:

- a) the Cr-L X-ray emission line coincides with the C- $K\alpha$ emission peak, so that the calculated carbon concentration could be a little bit too high;
- b) intensity measurements of light elements, like carbon, have to be performed in an integral fashion (14), which means that the total area of the emission peak should be measured instead of the intensity at the maximum. For each binary carbide this would mean long and tedious C- $K\alpha$ measurements. This problem was solved by the introduction of a so-called Area/Peak (A/P) factor, which represents the ratio between the (true) Area k-ratio and the peak k-ratio. The A/P factor for TiC_{1-x} in the expected composition range was determined in very pure TiC_{1-x} alloys (14), so that for later measurements in TiC_{1-x} coatings it would suffice to measure the peak K-ratio, which can then be converted to the area k-ratio using the A/P factor. The problem in TiC_{1-x} containing other (binary) carbides as impurities is that the A/P factor will be different from the A/P factor for pure TiC_{1-x} . Our solutions to these problems are not within the scope of this paper, but will be described in a separate publication (15).

In fig. 5 composition measurements (only carbon concentrations) in TiC_{1-x} coatings grown without carbon in the gas phase are compared to the TiC_{1-x} compositions found in equilibrated diffusion couples. All TiC_{1-x} compositions were related to the carbon content in the $Fe_{100-y}C_y$ substrate, and were determined at the centre of the TiC_{1-x} layer. In diffusion couples TiC_{1-x} compositions (very) near the TiC_{1-x}/Ti boundary are difficult to

measure by EPMA, but are found in accordance to the phase diagram (3,4).

As is obvious from fig. 5 all TiC_{1-x} CVD coatings are richer in carbon by 1.5 to 2.0 at.%. Both series of measurements show for the TiC_{1-x} stoichiometry only small dependencies of the substrate composition. An explanation for this is that in each case a slightly different composition of TiC_{1-x} will be in equilibrium at the $TiC/Fe_{100-y}Cy$ boundary with the substrate, when the substrate carbon content is varied. Or in other words: the course of the diffusion path starting from the substrate is dependent on the substrate composition and will determine the eventual TiC_{1-x} stoichiometry.

In the TiC_{1-x} formed in diffusion couples an iron content ranging between 0.5 and 1.3 at.% was found, in accordance with phase diagram results (4).

In case of TiC_{1-x} growth in standard industrial CVD facilities the coatings will invariably contain large amounts of impurities; we found iron and chromium concentrations between 1 and 4 at.%, oxygen and chlorine contents between 0 and 1 at.% (all determined by EPMA). The first two impurities mentioned were concentrated near the substrate/ TiC_{1-x} boundary. This probably means that nucleation of chromium (and iron) which is present as an impurity (chromium chloride) in the gas stream is favoured during the first minutes of the deposition.

Possibly TiC_{1-x} composition in these CVD coatings is influenced by the impurity content, chromium and iron possibly present at Ti-sites in the Ti-sublattice (so that a different diffusion path is followed), which would explain the differences observed between diffusion couples and CVD grown material in fig. 5. It is surprising that both in case of the equilibrated diffusion couples (44.5-45.5 at.%) and in the CVD case (45.5-47.5 at.%) a non-stoichiometric composition of TiC_{1-x} is found. An explanation for this observation on the basis of structure-binding-diffusion relationships in the material titanium carbide is presented in the next section.

Structure and binding in titanium carbide

To study the material TiC_{1-x} itself, we prepared a dozen samples covering the composition range (by melting mixtures of the elemental powders using arc-melting techniques). The lattice constants of the resulting polycrystalline samples were determined as a function of composition (EPMA) by X-ray diffraction (Guinier camera), see fig. 6. Impurity content was lower than 0.2 wt.% oxygen and 0.1 wt.% nitrogen, as measured by LECO TC 136 instrumentation. The variation of lattice constants, showing a maximum between 44 and 47 at.% carbon is in accordance with literature findings (16).

The binding energy of the $Ti-2p_{3/2}$ level, which is involved in the binding between titanium and carbon, was measured by XPS (using $Mg K\alpha_{1,2}$ radiation). The resulting curve (fig. 7) shows a maximum binding energy for a TiC_{1-x} composition of about 44 at.% carbon. These findings were confirmed by soft X-ray emission spectroscopy techniques (using the electron microprobe), yielding the full width at half maximum of the $Ti-Ln/1$ emission line as function of TiC_{1-x} composition, see fig. 8. The form of this emission band is reflecting the band structure of the material (17). In this X-ray emission study on various of the TiC_{1-x} samples a minimum in emission is observed at a composition of about 46 at.% carbon. It is interesting that the observed maximum in binding energy is coinciding (within experimental accuracy) with the TiC_{1-x} composition with maximum lattice parameter (fig. 6) and maximum melting point (fig. 9). This leads us to the obvious conclusion that in diffusion couple experiments as well as in CVD experiments, a preferential composition of TiC_{1-x} is formed which is thermodynamically

cally most stable, and which contains a minimum of lattice vacancies (maximum lattice constant).

This implies that in general it will not be easy to grow perfectly stoichiometric TiC_{1-x} layers by CVD, at least when equilibrium situations are used, and in case of substrates comparable to those we studied. An important implication is also that it is expected to be very difficult, if not impossible, to monitor TiC_{1-x} physical properties by changing the composition of TiC_{1-x} deposited layers over a broad composition range, if these layers are grown under situations of thermodynamic equilibrium, and in case of substrates compared to those we have used (e.g. plain carbon steels, not containing any alloying elements)!

In case no carbon is present in the gas phase during CVD experiments, the rate limiting step in TiC_{1-x} growth is carbon diffusion in the TiC_{1-x} surface layer (1,2). We found that in CVD experiments and in diffusion couple experiments TiC_{1-x} is formed in a preferential composition, which is thermodynamically the most stable one and the one containing a minimum of vacancies. If carbon diffusion in titanium carbide is proceeding by a vacancy mechanism this would mean that the diffusion coefficient of carbon in TiC_{1-x} of this preferential composition is minimal. This is in clear contradiction with the relatively flat carbon diffusion profile observed in TiC_{1-x} (diffusion couples) which indicates a maximum diffusion coefficient at the preferential composition. To see whether short-circuit diffusion is responsible for this we are investigating now some selected diffusion couples, in which the whole composition range of TiC_{1-x} is present. The results of this research will be reported in due course.

Acknowledgements:

We greatly acknowledge the help of Mr. Verspui and Ir. Michorius of Philips CMT Eindhoven, The Netherlands, when using their CVD equipment.

We are indebted to Mr. van den Dool of LECO Co., Ubach over Worms, The Netherlands, for performing oxygen and nitrogen analyses in TiC_{1-x} samples.

The investigations were supported in part by the Netherlands Foundation for Chemical Research (SON) with financial aid from the Netherlands Organization for the Advancement of Pure Research (ZWO).

References

- (1) P.P.J. Ramaekers, F.J.J. van Loo, Proc. of the 4th European Conference on CVD, J. Bloem, G. Verspui, L. Wolff (eds.), Eindhoven 1983, 546.
- (2) P.P.J. Ramaekers, G.F. Bastin and F.J.J. van Loo, Proc. of the 10th Intern. Symposium on the Reactivity of Solids, Dijon 1984, to be published by Elsevier Amsterdam in 1985.
- (3) P.P.J. Ramaekers, G.F. Bastin and F.J.J. van Loo, Z. Metallkde. 75 (1984) 639.
- (4) P.P.J. Ramaekers, F.J.J. van Loo and G.F. Bastin, Z. Metallkde. 76 (1985), accepted for publication in the April issue.
- (5) J.S. Kirkaldy and L.C. Brown, Can. Metall. Q. 3 (1963) 89.
- (6) J.B. Clark, Trans. Metall. Soc. A.I.M.E. 227 (1963) 1250.
- (7) J. Maas, G.F. Bastin, F.J.J. van Loo and R. Metselaar, Z. Metallkde. 74 (1983) 294.
- (8) J.H. Maas, Thesis, Eindhoven University of Technology, 1979.
- (9) G. Wassermann, J. Gerwen, Texturen Metallischer Werkstoffe, 2nd Edition, Springer-Verlag Berlin 1962.
- (10) U. Kobbe and H. Schuon, Siemens Zeitschrift 47 (1973) 119.

- (11) C.A. Wallace and R.C.C. Ward, *J. Appl. Cryst.* 8 (1975) 255.
- (12) R.F. Bunshah in: *Deposition Technologies for Films and Coatings*, Noyes Publications 1982, 139.
- (13) G.F. Bastin, F.J.J. van Loo and H.J.M. Heijligers, *X-Ray Spectrometry* 13 (1984) 91.
- (14) G.F. Bastin and H.J.M. Heijligers, *Microbeam Analysis*, A.D. Romig Jr. and J.I. Goldstein (eds.), San Francisco Press Inc. 1984, 291.
- (15) W.G. Sloof, Th.H. de Keijser, R. Delhez, P.P.J. Ramaekers and G.F. Bastin, to be published.
- (16) E.K. Storms: *The Refractory Carbides* (Academic Press Inc, New York), 1967, 8.
- (17) L. Ramqvist, K. Hamrin, G. Johansson, A. Fehlman, C. Nordling, *J. Phys. Chem. Solids* 1969, 1835.

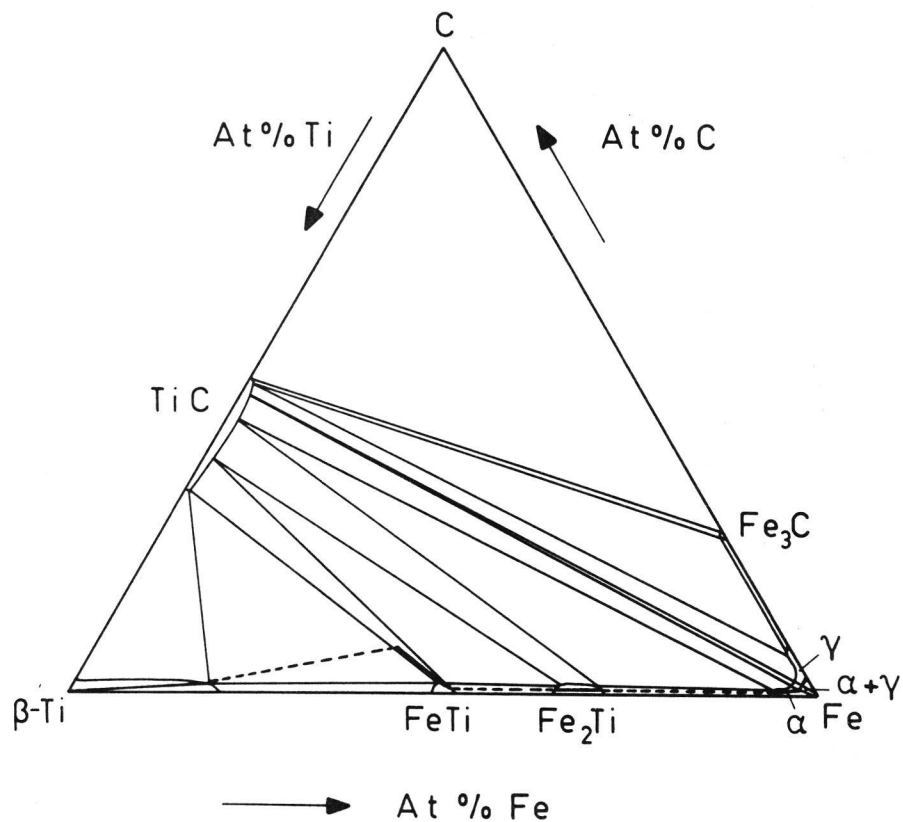


Figure 1: Observed diffusion path for couples $Ti-Fe_{100-y}C_y$, $0.2 < y < 6.5$

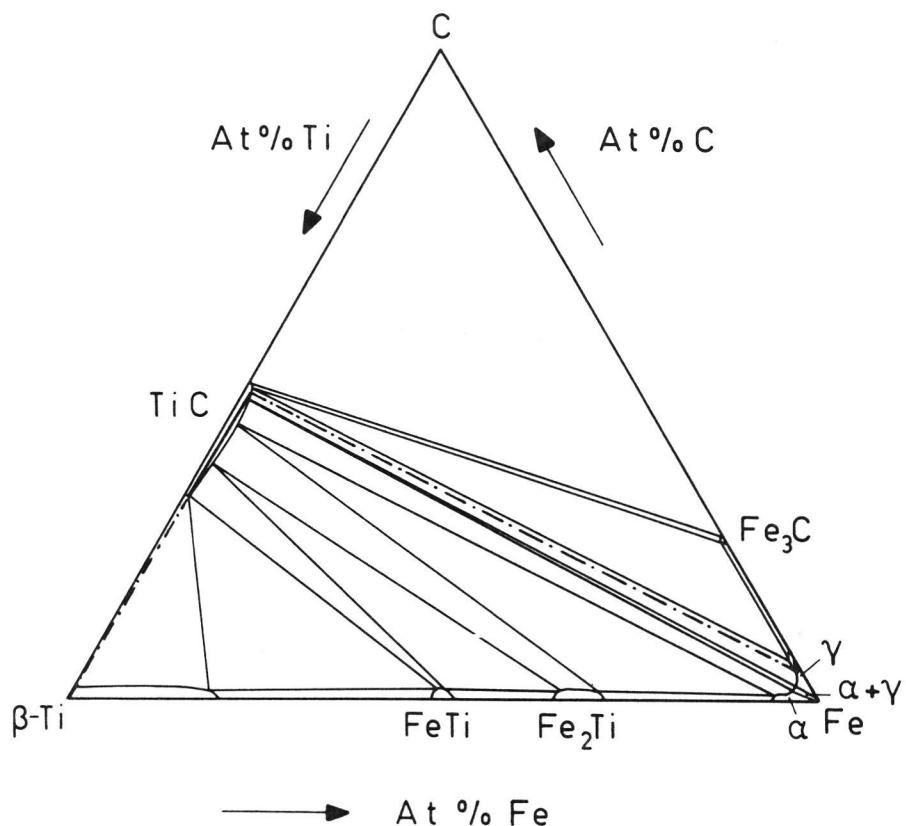


Figure 2: Observed diffusion path for couples $\text{Ti-Fe}_{100-y}\text{C}_y$, $y > 6.5$.

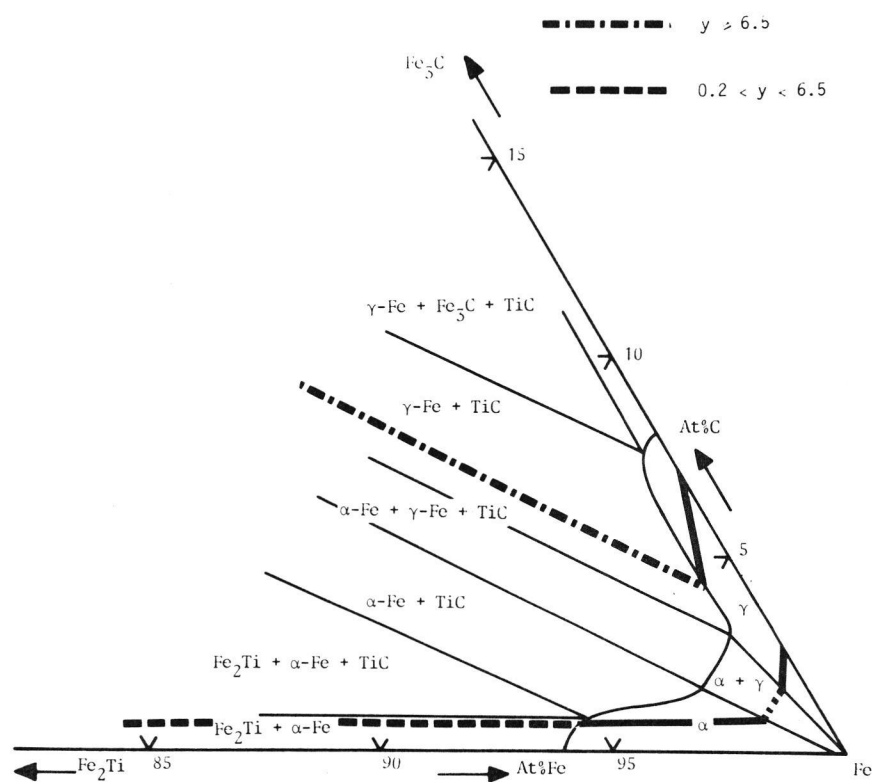


Figure 3: Enlargement of a section of Figs. 1 and 2, showing the decarburisation of $\text{Ti-Fe}_{100-y}\text{C}_y$ couples with $y > 0.2$.

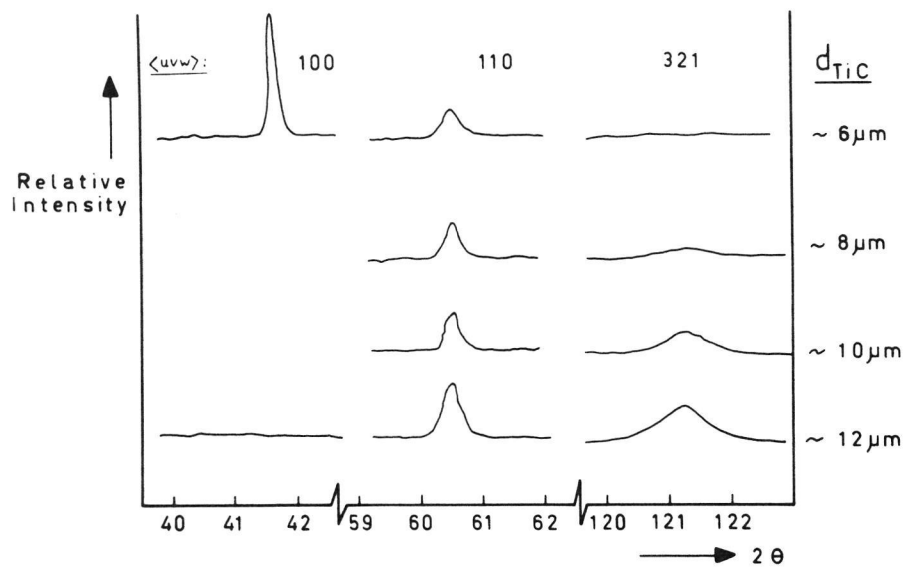


Figure 4: Observed X-ray diffraction pattern of CVD-grown TiC coating (no carbon source in the gas phase) after various grinding stages.

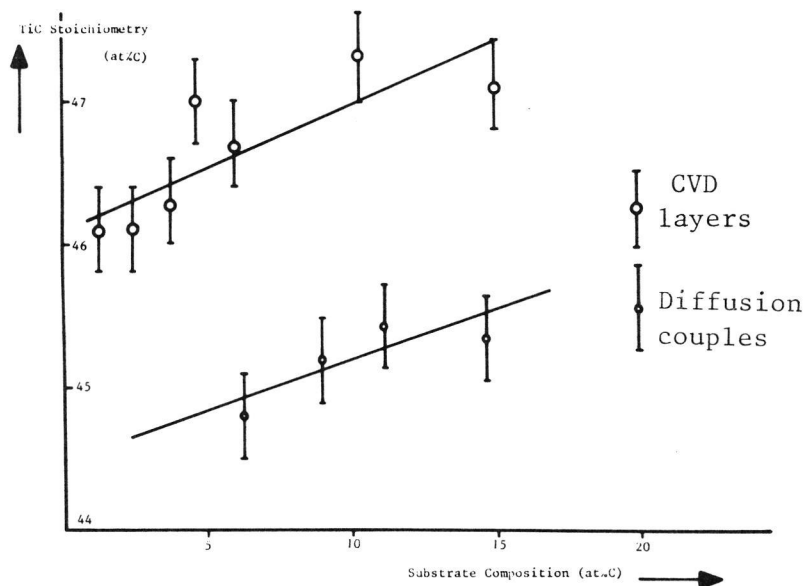


Figure 5: Relation between substrate composition and TiC_{1-x} stoichiometry in $\text{Ti-Fe}_{100-y}\text{C}_y$ diffusion couples and in CVD-coated $\text{Fe}_{100-y}\text{C}_y$.

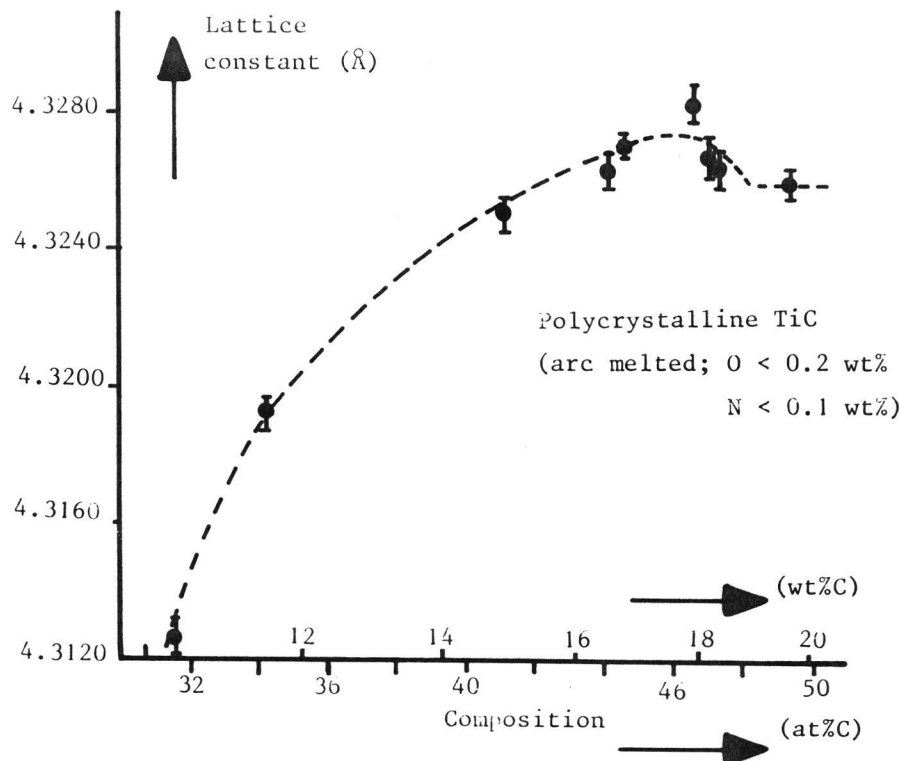


Figure 6: Lattice constants of polycrystalline TiC_{1-x} as a function of composition.

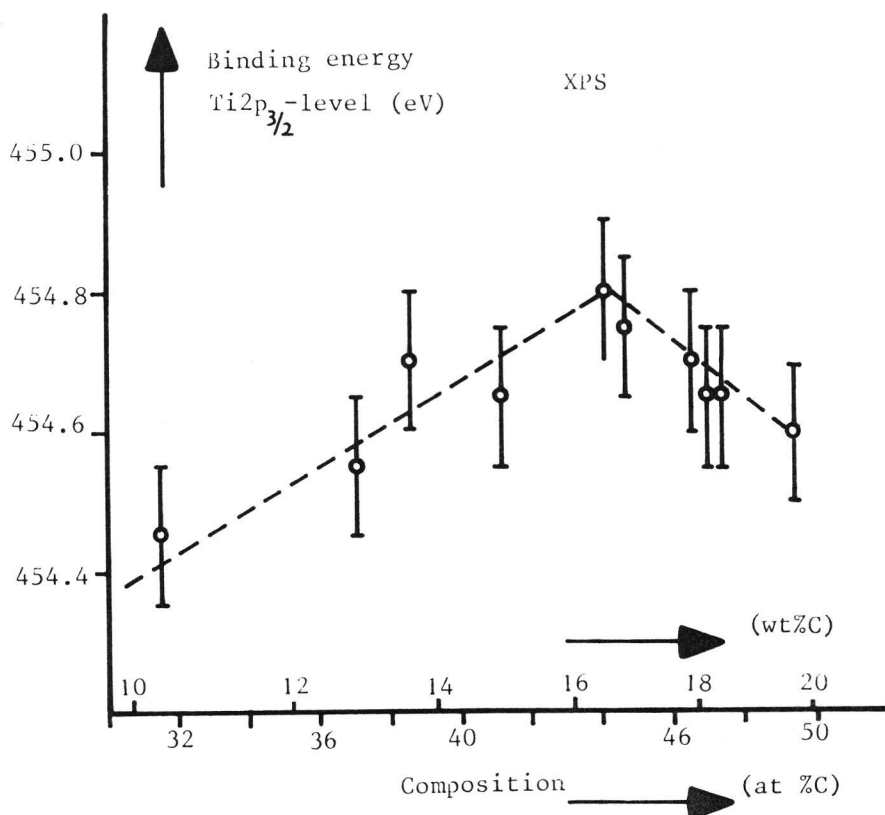


Figure 7: Binding energy of $\text{Ti} 2\text{p}_{3/2}$ -level in polycrystalline TiC_{1-x} as measured by XPS, vs. composition.

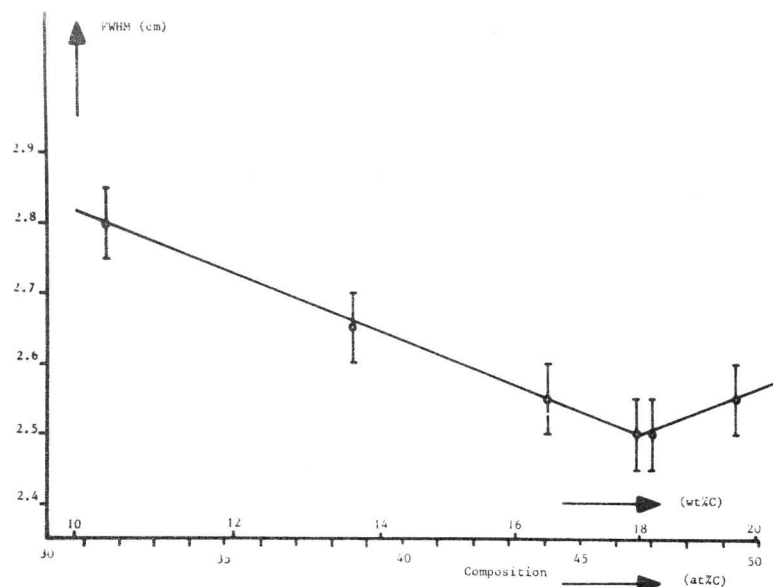


Figure 8: Half width (FWHM) for Ti-Ln/L1 X-ray emission in polycrystalline TiC_{1-x} vs. composition.

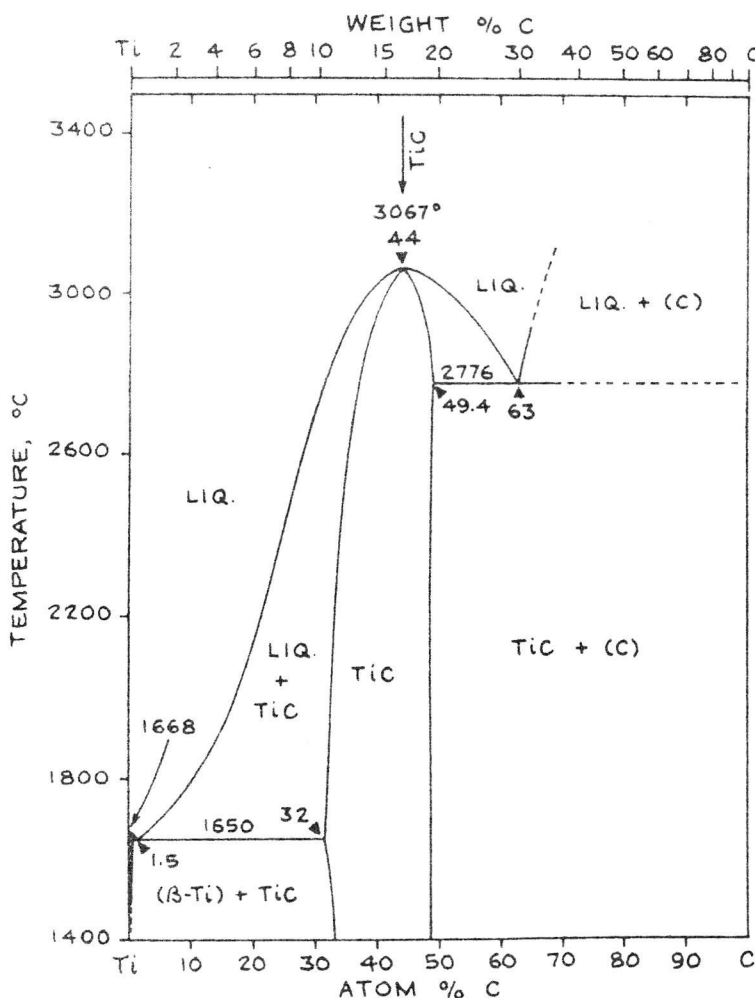


Figure 9: Phase diagram of the Ti-C system after E.Rudy (AFML-TR-65-2, 1969)